Liquid Saturation Data in Trickle Beds Operating Under Elevated Pressure

Faïcal Larachi, André Laurent, Noël Midoux, and Gabriel Wild
Laboratoire des Sciences du Génie Chimique, CNRS-ENSIC-INPL, BP 451, 54001 Nancy cédex, France

Liquid saturation in trickle-bed reactors plays a fundamental role in hydrodynamics as well as in mass and heat transfer. From the hydrodynamic viewpoint, it is affected strongly by the flow regime occurring in the reactor. Even though hydrotreating processes require an appreciable liquid saturation, prohibitive pressure drops should be avoided. Therefore, the reactors are often operated in the transition between trickling and pulsing regime. Liquid saturation also affects both wetting efficiency and mass transfer: high liquid saturations are needed for the processes in which reaction occurs exclusively on the wetted catalyst. However, a lower value is desirable if both gas-solid and liquid-solid reactions can occur (hydrogenation of benzene). Furthermore, numerous reactions are exothermic, for which the knowledge of liquid saturation becomes necessary to prevent hot spots and runaway.

There has been a large amount of research dealing with determining liquid saturation in laboratory-scale reactors at atmospheric pressure, but investigations on trickle beds operating at high pressures are rather scarce (Kohler and Richarz, 1985; Abbott et al., 1967; Wammes et al., 1990a, 1991). The maximum pressure investigated by these authors does not exceed 6 MPa; the flow regime used by Wammes et al. (1991) was trickling flow, but their other research (Wammes et al., 1990b) on liquid saturation at the transition between pulse flow and trickle flow regimes reports up to 2 MPa in pressure.

Our previous research (Hasseni et al., 1987) on single-phase and two-phase pressure drop in a trickle-bed reactor (cold mock-up: 1.0-m high, 23-mm-ID) showed pressures up to 10.1 MPa. To implement the hydrodynamic study of such reactors, we present here liquid saturation data (about 800 experiments) obtained by a tracer injection technique based on the conductimetric principle with several gas-liquid systems (with aqueous, organic, foaming and nonfoaming liquids; helium and nitrogen being the working gases) at pressures from the atmospheric pressure to 8.1 MPa. The experiments cover both trickling flow and high-interaction flow (i.e., pulsing regime), as well as the transition between them.

Apparatus and Procedure

Figure 1 shows the experimental apparatus used in this study.

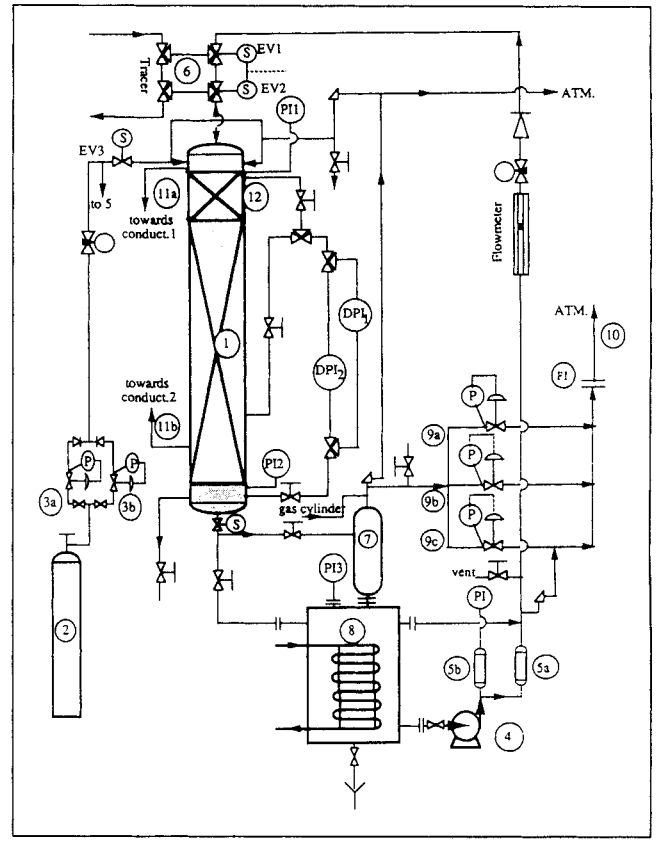

Figure 1. Experimental plant.

1.	Reactor	9a,b,c.	Gas upstream pressure controller
2.	Gas supply		
3a,b.	Pressure reducers	10.	Gas flowmeter
4.	Volumetric pump	11a,b.	Conductivity probes
5a,b.	Damping devices	12.	Transparent window
6.	Tracer injection loop	EV1,2,3.	Electronic valves
7.	Cyclonic gas/liquid separator	DP1,2.	Differential pressure transducers
8.	Liquid feed tank		

The reactor (1), with an inside diameter of 23 mm and a packed height of 1.0 m, consists of five stainless steel tubes connected to one another by flanges. The plant is capable of withstanding pressures up to 12 MPa. The uppermost tube, with a trans-

parent section (12) for visual observations of the flow, consists of two windows made of 50-mm-thick plexiglas. Two conductimetric probes (11a and 11b) are inserted at the top and bottom of the column (distance 915 mm). They consist of two stainless steel rods (electrodes) whose length is equal to the column radius; they are insulated by a polypropylene seal from the tube wall (counter electrode). The liquid is pumped by a reciprocating proportioning pump (4) and enters the column axially. The gas (nitrogen or helium) is supplied from a rack of gas cylinders (2) at 20 MPa; before entering radially into the reactor, it undergoes an expansion via pressure reducers (3a and 3b) and flows cocurrently downward with the liquid throughout a packing of glass beads of 2-mm-dia. and 38% porosity. To ensure a good radial distribution of the liquid at the top of the bed, an additional 10-cm-high packed element packed with 3-mm glass beads is provided. The gas and the liquid are separated in the cyclonic separator (7): the liquid is returned to the feed tank (8), while the gas is vented to the atmosphere after its passage by the gas upstream pressure controllers (9). The tracer [aqueous or polar organic solutions of NaCl, $LiClO_4$ and $(C_4H_9)_4N(Br)$] is injected from the injection loop (6). The values of the electrical conductivity at each extremity of the bed given by two conductimeters are sampled and recorded on a personal computer by means of a data acquisition unit with a sampling rate of 5 to 10 Hz.

The pressure influence on liquid saturation, the coalescence phenomenon, and the gas and liquid flow rates are studied by using seven gas-liquid systems (water-nitrogen, water +1% ethanol-nitrogen, water +40% sucrose-nitrogen, ethanol-nitrogen, propylene carbonate-nitrogen, propylene carbonate-helium, and ethylene glycol-nitrogen). The absolute pressure range investigated is 0.2–8.1 MPa at ambient temperature (293 to 298 K). The reactor was operated both in the trickling and the pulsing regimes, as well as in the transition between them. In fact, the data concerning the effect of the operating pressure on the displacement of the boundaries delimiting the different flow regimes are rather scanty (Hasseni et al., 1987; Wammes et al., 1990a, b). It seems, however, that for a given liquid mass flow rate, the transition between pulsing and trickling flow regimes occurs at higher gas mass flow rates, when the pressure is increased.

Results and Discussion

Calculation method

The tracer injection technique used here (imperfect pulse method with two downstream detection points) (Aris, 1959) allows us to estimate the total liquid saturation (Shah, 1979), which reduces to the external part (dynamic and static) in the case of a nonporous packing. For nonvolatile tracers, the total liquid saturation β is related to the liquid space time τ by the following equation:

$$\beta = \frac{L\tau}{\epsilon \rho_L Z} \tag{1}$$

τ can be evaluated by the convolution method. The convolution product of the theoretical impulse response (E) and the measured inlet signal (x) is calculated, and the difference between the function thus obtained and the outlet experimental signal (y) is then minimized by nonlinear fitting (Box's complex algorithm) using the following quadratic objective function (for each run, about 100 points are selected in the summation):

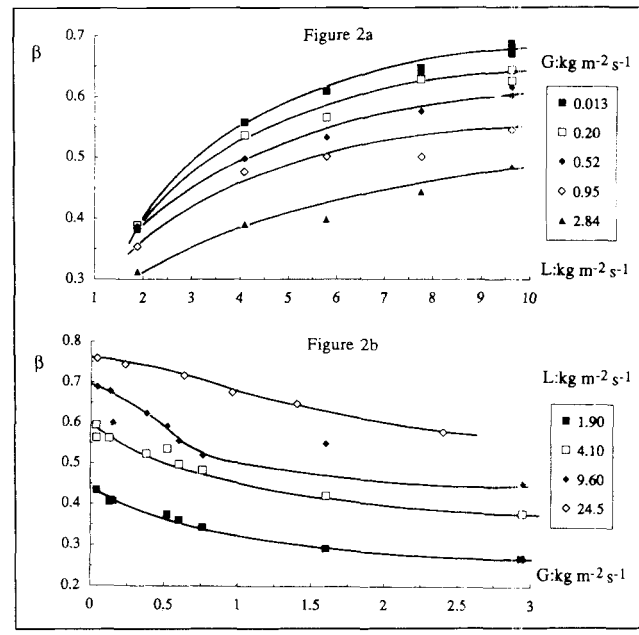

Figure 2. Influence of gas and liquid mass flow rates on total liquid saturation for water-nitrogen at 8.1 and 5.1 MPa.

$$\sigma^2 = \sum_k \left(y(t_k)^{\exp} - \int_0^{t_k} x(v)^{\exp} E(t_k - v)\, dv \right)^2 \tag{2}$$

The plug-flow model with axial dispersion in a column open to dispersion is used for this purpose, the corresponding impulse response being (Nauman and Buffham, 1983):

$$E(\theta) = \frac{1}{2}\sqrt{\frac{\mathrm{Pe}}{\pi\theta^3}} \exp\left(-\frac{\mathrm{Pe}(1-\theta)^2}{4\theta}\right) \tag{3}$$

For the packing size and the column height used in this work, it should be noted that the liquid flows practically without axial dispersion with the values of axial Péclet number *Pe* at least equal to 100.

The experiments were repeated up to five times and seem to be reproducible within 5 to 10%. Provided the calibration relationship between the tracer concentration and the apparent electrical conductivity is linear, the tracer technique seems to be more advantageous compared with other techniques (the drainage method, for instance), since it provides an on-line estimation of liquid saturation without any interruption of the flow. This technique, however, is not a workable method when the flow regime occurring is the spray flow: because the liquid is dispersed in fine droplets independent of one another, liquid saturation becomes underestimated.

Influence of gas and liquid throughputs on β

Figures 2a and 2b show the influence of both gas and liquid superficial mass flow rates on total liquid saturation for the system: water-nitrogen at 8.1 and 5.1 MPa, respectively. At any pressure, liquid saturation increases with the increase in

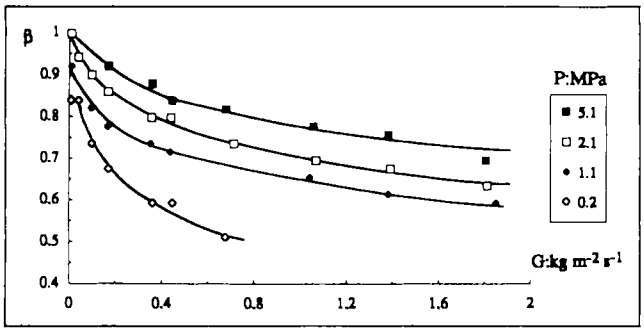

Figure 3. Influence of operating pressure on total liquid saturation for ETG-nitrogen (L = 13.2 kg·m^{-2}·s^{-1}).

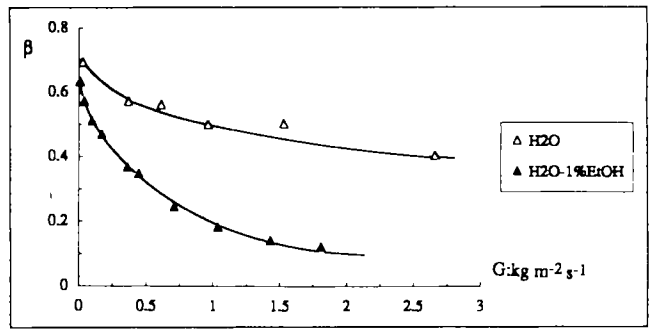

Figure 5. Influence of foaming on total liquid saturation for two aqueous systems at 1.1 MPa (L = 13.2 kg·m^{-2}·s^{-1}).

liquid mass flow rate and decreases with the increase in gas mass flow rate. At a given liquid flow rate (Figure 2b), it first decreases rapidly when a small gas mass flow rate is introduced and becomes approximately constant when the gas flow rate is high. The same trend is observed at 8.1 MPa where β is plotted vs. L for different values of G. At first, an abrupt increase of β is noticed for low liquid flow rates followed by a slight augmentation at high values of L. Similar observations were reported by Blok and Drinkenburg (1982) from experiments conducted at atmospheric pressure. These authors ascribed the quasi constancy of liquid saturation to the appearance of the pulsing flow regime.

Influence of the total pressure on β

Figure 3 shows the pressure influence on liquid saturation as a function of the gas mass flow rate and fixed liquid flow rate for the ethylene glycol-nitrogen system, from 0.2 to 5.1 MPa. It appears that, for the given gas and liquid mass flow rates, an increase in total pressure increases liquid saturation. This can be explained by the fact that the same gas mass flow rate would occupy less space under elevated pressure. Furthermore, since the decrease in the gas superficial velocity leads to less interfacial interactions between the gas and the liquid, the mean residence time of the liquid phase becomes longer. Note that beyond 2.1 MPa and extremely low gas flow rates, the column is practically filled with ETG (ethylene glycol) due to its relatively high viscosity (18 mPa•s at 298 K).

Figure 4 (the propylene carbonate-nitrogen system) shows that β is pressure-independent for very low gas velocities ($u_G \leq 1$ cm/s). Such an observation implies that it is not necessary to measure liquid saturations under high pressure, provided that gas velocities remain sufficiently low. Measurements carried out at atmospheric pressure and the same velocities would lead to identical values of β. However, even in the trickle-flow regime and gas superficial velocity of a few cm/s, liquid saturation depends on the operating pressure. Wammes et al. (1991) reported the same behavior and stressed on the risks of extrapolation from ambient pressure data to high-pressure conditions.

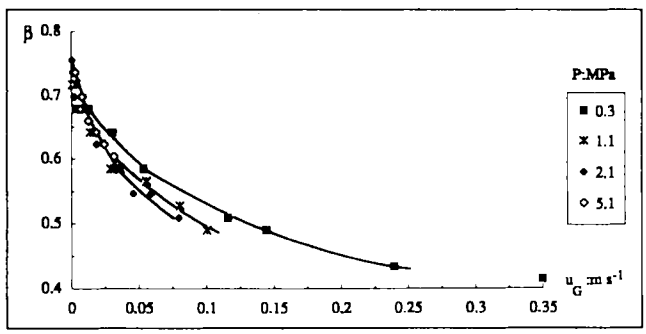

Figure 4. Total liquid saturation vs. gas superficial velocity at various pressures for PC-nitrogen (L = 13.2 kg·m^{-2}·s^{-1}).

Influence of the coalescence phenomenon on β

The influence of foaming on liquid saturation was also studied with two aqueous systems water–nitrogen (coalescent) and water + 1% ethanol–nitrogen (foaming) (Figure 5). Liquid saturation is much smaller for foaming liquids than for coalescing liquids, regardless of the reactor pressure. Actually, no quantitative models are available that characterize the coalescence inhibition phenomena of hydrodynamics as well as mass transfer behaviors of such contactors. However, the low liquid saturation values observed, when the gas-liquid system foams, can be attributed to the high stability of fine bubbles fixed on and between the solid particles, which reduces the difference in the linear velocities of the gas and the liquid in the usual range of fluid throughputs of trickle beds. Moreover, it is experimentally observed that an increase in pressure shifts the initial foaming flow toward higher mass flow rates where pressure fluctuations of several bars were observed.

Acknowledgment

The authors are grateful to the Institut Français du Pétrole and the Algerian Ministère aux Universités for the financial support of this work.

Literature Cited

Abbott, M. D., G. R. Moore, and J. L. Ralph, *Proc. ABG Conf.*, paper S4, (1967).

Aris, R., "Notes on the Diffusion-Type Model for Longitudinal Mixing in Flow," *Chem. Eng. Sci.*, **9**, 266 (1959).

Blok, J. R., and A. A. H. Drinkenburg, "Hydrodynamics and Mass Transfer in Pulsing Trickle-Bed Columns," *ACS Symp. Ser.*, No. 196, *Chemical Reaction Engineering*, Washington, DC, p. 393 (1982).

Hasseni, W., A. Laurent, N. Midoux, and J. C. Charpentier, "Régimes d'Écoulement dans un Réacteur Catalytique à Lit Fixe Arrosé Fonctionnant à Cocourant de Gaz et de Liquide vers le Bas," *Entropie*, **137/138**, 127 (1987).
Kohler, M., and W. Richarz, "Investigation of Liquid Holdup in Trickle-Bed Reactors," *Ger. Chem. Eng.*, **8**, 295 (1985).
Nauman, E. B., and B. A. Buffham, "Mixing in Continuous Flow Systems," Wiley Interscience (1983).
Shah, Y. T., *Gas-Liquid-Solid Reactor Design*, McGraw-Hill, New York (1979).
Wammes, W. J. A., S. J. Mechielsen, and K. R. Westerterp, "The Influence of the Reactor Pressure on the Hydrodynamics in a Cocurrent Gas-Liquid Trickle-Bed Reactor," *Chem. Eng. Sci.*, **45**, 2247 (1990a).
Wammes, W. J. A., S. J. Mechielsen, and K. R. Westerterp, "The Transition between Trickle Flow and Pulse Flow in a Cocurrent Gas-Liquid Trickle-Bed Reactor at Elevated Pressure," *Chem. Eng. Sci.*, **45**, 3149 (1990b).
Wammes, W. J. A., S. J. Mechielsen, and K. R. Westerterp, "The Influence of Pressure on the Liquid Hold-up in a Cocurrent Gas-Liquid Trickle-Bed Reactor Operating at Low Gas Velocities," *Chem. Eng. Sci.*, **46**, 409 (1991).

Notation

$E(t)$ = impulse response of the system, s^{-1}
G = gas superficial mass flow rate, $kg \cdot m^{-2} \cdot s^{-1}$
L = liquid superficial mass flow rate, $kg \cdot m^{-2} \cdot s^{-1}$
P = operating pressure, MPa
Pe = axial Péclet number based on actual velocity
t, t_k = time, s
u = superficial velocity, $m \cdot s^{-1}$
v = variable in Eq. 2
x = reduced inlet conductivity signal
y = reduced outlet conductivity signal
Z = packed height, m

Greek letters

β = liquid saturation (volume of liquid/porous volume)
ϵ = bed porosity
ρ = density, $kg \cdot m^{-3}$
σ^2 = objective function
τ = space time, s
θ = dimensionless time, t/τ

Subscripts

G = gas
L = liquid

Superscripts

exp = experimental

Manuscript received Nov. 14, 1990, and revision received Apr. 29, 1991.